

Self-supervised Learning is More Robust to Dataset Imbalance

Hong Liu ^{*} Jeff Z. HaoChen [†] Adrien Gaidon [‡] Tengyu Ma [§]

May 24, 2022

Abstract

Self-supervised learning (SSL) is a scalable way to learn general visual representations since it learns without labels. However, large-scale unlabeled datasets in the wild often have long-tailed label distributions, where we know little about the behavior of SSL. In this work, we systematically investigate self-supervised learning under dataset imbalance. First, we find out via extensive experiments that off-the-shelf self-supervised representations are already more robust to class imbalance than supervised representations. The performance gap between balanced and imbalanced pre-training with SSL is significantly smaller than the gap with supervised learning, across sample sizes, for both in-domain and, especially, out-of-domain evaluation. Second, towards understanding the robustness of SSL, we hypothesize that SSL learns richer features from frequent data: it may learn label-irrelevant-but-transferable features that help classify the rare classes and downstream tasks. In contrast, supervised learning has no incentive to learn features irrelevant to the labels from frequent examples. We validate this hypothesis with semi-synthetic experiments and theoretical analyses on a simplified setting. Third, inspired by the theoretical insights, we devise a re-weighted regularization technique that consistently improves the SSL representation quality on imbalanced datasets with several evaluation criteria, closing the small gap between balanced and imbalanced datasets with the same number of examples.

1 Introduction

Self-supervised learning (SSL) is an important paradigm of machine learning, because it can leverage the availability of large-scale unlabeled datasets to learn representations for a wide range of downstream tasks and datasets [He et al., 2020, Chen et al., 2020, Grill et al., 2020, Caron et al., 2020, Chen and He, 2021]. Current SSL algorithms are mostly trained on curated, balanced datasets, but large-scale unlabeled datasets in the wild are inevitably imbalanced with a long-tailed label distribution [Reed, 2001, Liu et al., 2019]. Curating a class-balanced unlabeled dataset requires the knowledge of labels, which defeats the purpose of leveraging unlabeled data by SSL.

The behavior of SSL algorithms under dataset imbalance remains largely underexplored in the literature, but extensive studies do not bode well for supervised learning (SL) with imbalanced datasets. The performance of vanilla supervised methods degrades significantly on class-imbalanced datasets [Cui et al., 2019, Cao et al., 2019, Buda et al., 2018], posing challenges to practical applications such as instance segmentation [Tang et al., 2020] and depth estimation [Yang et al., 2021]. Many recent works address this issue with various regularization and re-weighting/re-sampling techniques [Ando and Huang, 2017, Wang et al., 2017b, Jamal et al., 2020, Cui et al., 2019, Cao et al., 2019, 2021, Tian et al., 2020, Hong et al., 2021, Wang et al., 2021].

In this work, we systematically investigate the representation quality of SSL algorithms under class imbalance. Perhaps surprisingly, we find out that off-the-shelf SSL representations are already more robust to dataset imbalance than the representations learned by supervised pre-training. We evaluate the representation

^{*}Stanford University, email: hliu99@stanford.edu

[†]Stanford University, email: jhaochen@stanford.edu

[‡]Toyota Research Institute, email: adrien.gaidon@tri.global

[§]Stanford University, email: tengyuma@stanford.edu

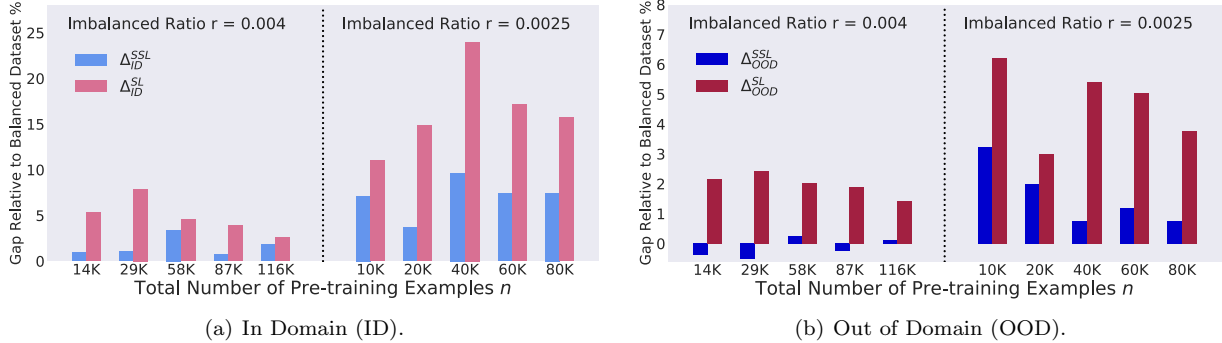


Figure 1: **Relative performance gap** (lower is better) between imbalanced and balanced representation learning. The gap is much smaller for self-supervised (MoCo v2) representations (Δ^{SSL} in blue) vs. supervised ones (Δ^{SL} in red) on long-tailed ImageNet with various number of examples n , across both ID (a) and OOD (b) evaluations. See Equation (1) for the precise definition of the relative performance gap and Figure 2 for the absolute performance.

quality by linear probe on in-domain (ID) data and finetuning on out-of-domain (OOD) data. We compare the robustness of SL and SSL representations by computing the gap between the performance of the representations pre-trained on balanced and imbalanced datasets of the same sizes. We observe that the balance-imbalance gap for SSL is much smaller than SL, under a variety of configurations with varying dataset sizes and imbalance ratios and with both ID and OOD evaluations (see Figure 1 and Section 2 for more details). This robustness holds even with the same number of samples for SL and SSL, although SSL does not require labels and hence can be more easily applied to larger datasets than SL.

Why is SSL more robust to dataset imbalance? We identify the following underlying cause to answer this fundamental question: SSL learns richer features from the frequent classes than SL does. These features may help classify the rare classes under ID evaluation and are transferable to the downstream tasks under OOD evaluation. For simplicity, consider the situation where rare classes have so limited data that both SL and SSL models overfit to the rare data. In this case, it is important for the models to learn diverse features from the frequent classes which can help classify the rare classes. Supervised learning is only incentivized to learn those features relevant to predicting frequent classes and may ignore other features. In contrast, SSL may learn the structures within the frequent classes better—because it is not supervised or incentivized by any labels, it can learn not only the label-relevant features but also other interesting features capturing the intrinsic properties of the input distribution, which may generalize/transfer better to rare classes and downstream tasks.

We empirically validate this intuition by visualizing the features on a semi-synthetic dataset where the label-relevant features and label-irrelevant-but-transferable features are prominently seen by design (cf. Section 3.2). In addition, we construct a toy example where we can rigorously prove the difference between self-supervised and supervised features in Section 3.1.

Finally, given our theoretical insights, we take a step towards further improving SSL algorithms, closing the small gap between SSL on balanced and imbalanced datasets. We identify the generalization gap between the empirical and population pre-training losses on rare data as the key to improvements.

To this end, we design a simple algorithm that first roughly estimates the density of examples with kernel density estimation and then applies a larger sharpness-based regularization [Foret et al., 2020] to the estimated rare examples. Our algorithm consistently improves the representation quality under several evaluation protocols.

We sum up our contributions as follows. (1) We are the first to systematically investigate the robustness of self-supervised representation learning to dataset imbalance. (2) We propose and validate an explanation of this robustness of SSL, empirically and theoretically. (3) We propose a principled method to improve SSL under unknown dataset imbalance.

2 Exploring the Effect of Class Imbalance on SSL

Dataset class imbalance can pose challenge to self-supervised learning in the wild. Without access to labels, we cannot know in advance whether a large-scale unlabeled dataset is imbalanced. Hence, we need to study how SSL will behave under dataset imbalance to deploy SSL in the wild safely. In this section, we systematically investigate the effect of class imbalance on self-supervised representations with experiments.

2.1 Problem Formulation

Class-imbalanced pre-training datasets. We assume the datapoints / inputs are in \mathbb{R}^d and come from C underlying classes. Let x denote the input and y denote the corresponding label. Supervised pre-training algorithms have access to the inputs and corresponding labels, whereas self-supervised pre-training only observes the inputs. Given a pre-training distribution \mathcal{P} over $\mathbb{R}^d \times [C]$, let r denote the ratio of class imbalance. That is, r is the ratio between the probability of the rarest class and the most frequent class: $r = \frac{\min_{j \in [C]} \mathcal{P}(y=j)}{\max_{j \in [C]} \mathcal{P}(y=j)} \leq 1$. We will construct distributions with varying imbalance ratios and use \mathcal{P}^r to denote the distribution with ratio r . We also use \mathcal{P}^{bal} for the case where $r = 1$, i.e. the dataset is balanced. Large-scale data in the wild often follow heavily long-tailed label distributions where r is small. We assume that for any class $j \in [C]$, the class-conditional distribution $\mathcal{P}^r(x|y=j)$ is the same across balanced and imbalanced datasets for all r . The pre-training dataset $\widehat{\mathcal{P}}_n^r$ consists of n i.i.d. samples from \mathcal{P}^r .

Pre-trained models. A feature extractor is a function $f_\phi : \mathbb{R}^d \rightarrow \mathbb{R}^m$ parameterized by neural network parameters ϕ , which maps inputs to representations. A linear head is a linear function $g_\theta : \mathbb{R}^m \rightarrow \mathbb{R}^C$, which can be composed with f_ϕ to produce the predictions. SSL algorithms learn ϕ from unlabeled data. Supervised pre-training learns the feature extractor and the linear head from labeled data. We drop the head and only evaluate the quality of feature extractor ϕ .¹

Following the standard evaluation protocol in prior works [He et al., 2020, Chen et al., 2020], we measure the quality of learned representations on both *in-domain* and *out-of-domain* datasets with either *linear probe* or *fine-tuning*, as detailed below.

In-domain (ID) evaluation tests the performance of representations on the *balanced in-domain* distribution \mathcal{P}^{bal} with **linear probe**. Given a feature extractor f_ϕ pre-trained on a pre-training dataset $\widehat{\mathcal{P}}_n^r$ with n data points and imbalance ratio r , we train a C -way linear classifier θ on top of f_ϕ on a *balanced* dataset² sampled i.i.d. from \mathcal{P}^{bal} . We evaluate the representation quality with the top-1 accuracy of the learned linear head on \mathcal{P}^{bal} . We denote the ID accuracy of supervised pre-trained representations by $A_{\text{ID}}^{\text{SL}}(n, r)$. Note that $A_{\text{ID}}^{\text{SL}}(n, 1)$ stands for the result with balanced pre-training dataset. For SSL representations, we denote the accuracy by $A_{\text{ID}}^{\text{SSL}}(n, r)$.

Out-of-domain (OOD) evaluation tests the performance of representations by *fine-tuning* the feature extractor and the head on a (or multiple) *downstream* target distribution \mathcal{P}_t . Starting from a feature extractor f_ϕ (pre-trained on a dataset of size n and imbalance ratio r) and a randomly initialized classifier θ , we fine-tune ϕ and θ on the target dataset $\widehat{\mathcal{P}}_t$, and evaluate the representation quality by the expected top-1 accuracy on \mathcal{P}_t . We use $A_{\text{OOD}}^{\text{SL}}(n, r)$ and $A_{\text{OOD}}^{\text{SSL}}(n, r)$ to denote the resulting accuracies of supervised and self-supervised representations, respectively.

Summary of varying factors. We aim to study the effect of class imbalance to feature qualities on a diverse set of configurations with the following varying factors: (1) the number of examples in pre-training n , (2) the imbalance ratio of the pre-training dataset r , (3) ID or OOD evaluation, and (4) self-supervised learning algorithms: MoCo v2 [He et al., 2020], or SimSiam [Chen and He, 2021].

¹It is well-known that the composition of the head and features learned from supervised learning is more sensitive to imbalanced dataset than feature extractor ϕ itself [Cao et al., 2019, Kang et al., 2020]. Please also see Table 3 in Appendix C for a comparison between CRT [Kang et al., 2020] and Supervised.

²We essentially use the largest balanced labeled ID dataset for this evaluation, which oftentimes means the entire curated training dataset, such as CIFAR-10 with 50,000 examples and ImageNet with 1,281,167 examples.

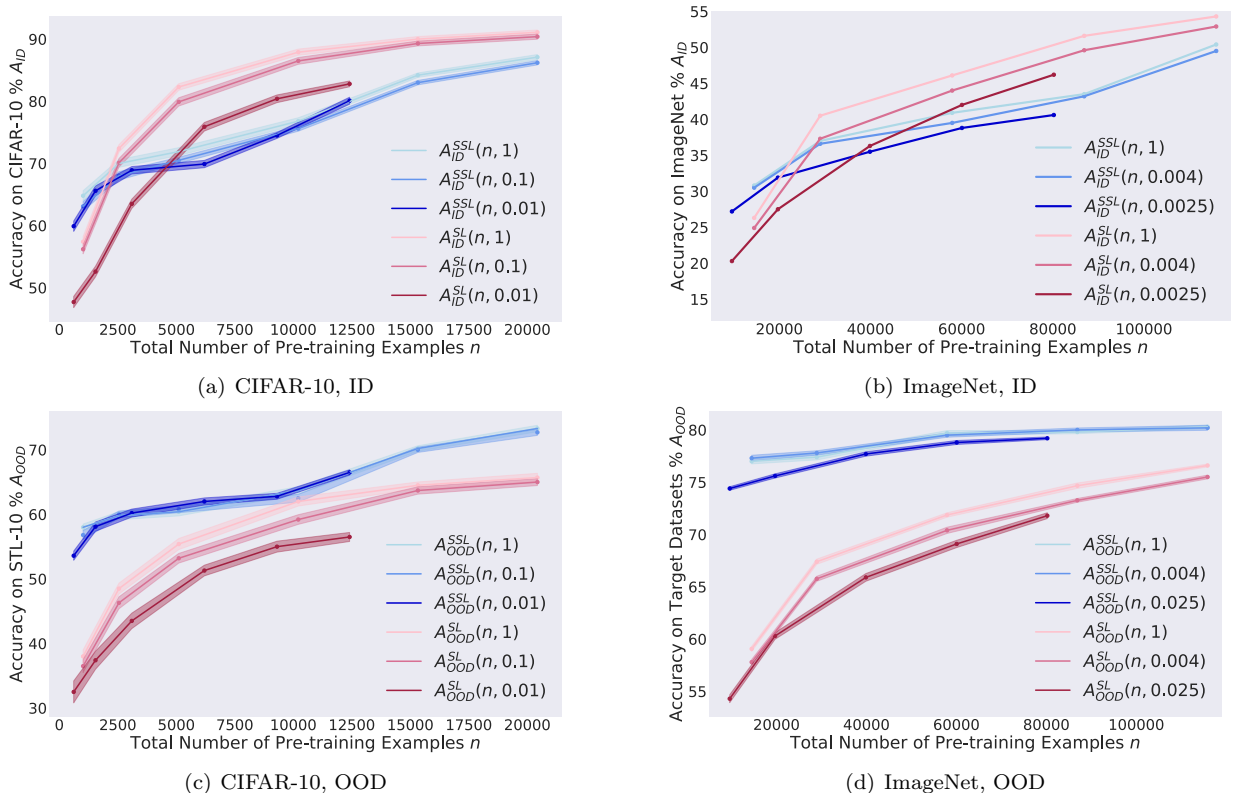


Figure 2: **Representation quality on balanced and imbalanced datasets.** Left: CIFAR-10, SL vs. SSL (SimSiam); Right: ImageNet, SL vs. SSL (MoCo v2). For both ID and OOD, the gap between balanced and imbalanced datasets with the same n is larger for supervised learning. The accuracy of supervised representations is better with reasonably large n in ID evaluation, while self-supervised representations perform better in OOD evaluation.⁴

2.2 Experimental Setup

Datasets. We pre-train the representations on variants of ImageNet [Russakovsky et al., 2015] or CIFAR-10 [Krizhevsky and Hinton, 2009] with a wide range of numbers of examples and ratios of imbalance. Following Liu et al. [2019], we consider exponential and Pareto distributions, which closely simulate the natural long-tailed distributions. We consider imbalance ratio in $\{1, 0.004, 0.0025\}$ for ImageNet and $\{1, 0.1, 0.01\}$ for CIFAR-10. For each imbalance ratio, we further downsample the dataset with a sampling ratio in $\{0.75, 0.5, 0.25, 0.125\}$ to form datasets with varying sizes. Note that we fix the variant of the dataset when comparing different algorithms. For ID evaluation, we use the original CIFAR-10 or ImageNet training set for the training phase of linear probe and use the original validation set for the final evaluation. For OOD evaluation of representations learned on CIFAR-10, we use STL-10 [Coates et al., 2011] as the target /downstream dataset. For OOD evaluation of representations learned on ImageNet, we fine-tune the pre-trained feature extractors on CUB-200 [Wah et al., 2011], Stanford Cars [Krause et al., 2013], Oxford Pets [Parkhi et al., 2012], and Aircrafts [Maji et al., 2013], and measure the representation quality with average accuracy on the downstream tasks.

Models. We use ResNet-18 on CIFAR-10 and ResNet-50 on ImageNet as backbones. For supervised pre-training, we follow the standard protocol of He et al. [2016] and Kang et al. [2020]. For self-supervised pre-training, we consider MoCo v2 [He et al., 2020] and SimSiam [Chen and He, 2021]. We run each evaluation experiment with 3 seeds and report the average and standard deviation in the figures. Further implementation details and additional results are deferred to Section A.

2.3 Results: Self-supervised Learning is More Robust than Supervised Learning to Dataset Imbalance

In Figure 2, we plot the results of ID and OOD evaluations, respectively. For both ID and OOD evaluations, the gap between SSL representations learned on balanced and imbalanced datasets with the same number of pre-training examples, i.e., $A^{\text{SSL}}(n, 1) - A^{\text{SSL}}(n, r)$, is smaller than the gap of supervised representations, i.e., $A^{\text{SL}}(n, 1) - A^{\text{SL}}(n, r)$, consistently in all configurations. Furthermore, we compute the relative accuracy gap to balanced dataset $\Delta^{\text{SSL}}(n, r) \triangleq (A^{\text{SSL}}(n, 1) - A^{\text{SSL}}(n, r)) / A^{\text{SSL}}(n, 1)$ in Figure 1. We observe that with the same number of pre-training examples, the relative gap of SSL representations between balanced and imbalanced datasets is smaller than that of SL representations across the board,

$$\Delta^{\text{SSL}}(n, r) \triangleq \frac{A^{\text{SSL}}(n, 1) - A^{\text{SSL}}(n, r)}{A^{\text{SSL}}(n, 1)} \ll \Delta^{\text{SL}}(n, r) \triangleq \frac{A^{\text{SL}}(n, 1) - A^{\text{SL}}(n, r)}{A^{\text{SL}}(n, 1)}. \quad (1)$$

Also note that comparing the robustness with the same number of data is actually in favor of SL, because SSL is more easily applied to larger datasets without the need of collecting labels.

ID vs. OOD. As shown in Figure 2, we observe that representations from supervised pre-training perform better than self-supervised pre-training in ID evaluation with reasonably large n , while self-supervised pre-training is better in OOD evaluation. This phenomenon is orthogonal to our observation that SSL is more robust to dataset imbalance, and is consistent with recent works (e.g., Chen et al. [2020], He et al. [2020]) which also observed that SSL performs slightly worse than supervised learning on balanced ID evaluation but better on OOD tasks.

3 Analysis

We have found out with extensive experiments that self-supervised representations are more robust to class imbalance than supervised representations. A natural and fundamental question arises: where does the robustness stem from? In this section, we propose a possible reason and justify it with theoretical and empirical analyses.

SSL learns richer features from frequent data that are transferable to rare data. The rare classes of the imbalanced dataset can contain only a few examples, making it hard to learn proper features to classify the rare classes. In this case, one may want to resort to the features learned from the frequent classes for help. However, due to the supervised nature of classification tasks, the supervised model mainly learns the features that help classify the frequent classes and may neglect other features which can transfer to the rare classes and potentially the downstream tasks. Partly because of this, Jamal et al. [2020] explicitly encourage the model to learn features transferable from the frequent to the rare classes with meta-learning. In contrast, in self-supervised learning, without the bias or incentive from the labels, the models can learn richer features that capture the intrinsic structures of the inputs—both features useful for classifying the frequent classes and features transferable to the rare classes.

3.1 Rigorous Analysis on A Toy Setting

To justify the above conjecture, we instantiate supervised and self-supervised learning in a setting where the features helpful to classify the frequent classes and features transferable to the rare classes can be clearly separated. In this case, we prove that self-supervised learning learns better features than supervised learning.

Data distribution. Let e_1, e_2 be two orthogonal unit-norm vectors in the d -dimensional Euclidean space. Consider the following pre-training distribution \mathcal{P} of a 3-way classification problem, where the class label $y \in [3]$. The input x is generated as follows. Let $\tau > 0$ and $\rho > 0$ be hyperparameters of the distribution. First sample q uniformly from $\{0, 1\}$ and $\xi \sim \mathcal{N}(0, I)$ from Gaussian distribution. For the first class ($y = 1$), set $x = e_1 - q\tau e_2 + \rho\xi$. For the second class ($y = 2$), set $x = -e_1 - q\tau e_2 + \rho\xi$. For the third class ($y = 3$), set

⁴The maximum n is smaller for extreme imbalance. The standard deviation comes only from the randomness of evaluation. We do not include the stddev for ImageNet ID due to limitation of computation resources.

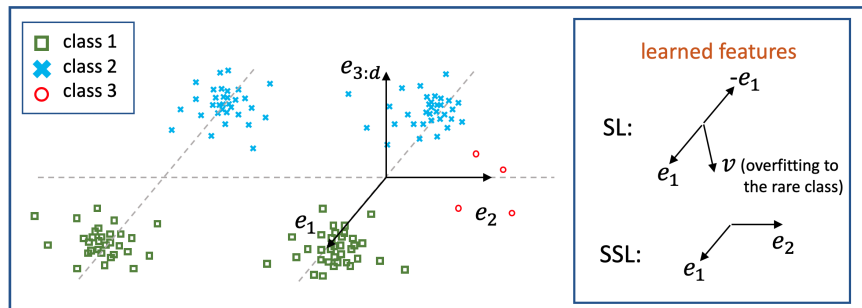


Figure 3: **Explaining SSL’s robustness in a toy setting.** e_1 and e_2 are two orthogonal directions in the d -dimensional Euclidean space that decides the labels, and $e_{3:d}$ represents the other $d - 2$ dimensions. Classes 1 and 2 are frequent classes and the third class is rare. To classify the three classes, the representations need to contain both e_1 and e_2 directions. Supervised learning learns direction e_1 from the frequent classes (which is necessary and sufficient to identify classes 1 and 2) and some overfitting direction v from the rare class which has insufficient data. Note that v might be mostly in the $e_{3:d}$ directions due to overfitting. In contrast, SSL learns both e_1 and e_2 directions from the frequent classes because they capture the intrinsic structures of the inputs (e.g., e_1 and e_2 are the directions with the largest variances), even though e_2 does not help distinguish the frequent classes. The direction e_2 learned from frequent data by SSL can help classify the rare class.

$x = e_2 + \rho\xi$. Classes 1 and 2 are frequent classes, while class 3 is the rare class, i.e., $\frac{\mathcal{P}(y=3)}{\mathcal{P}(y=1)}, \frac{\mathcal{P}(y=3)}{\mathcal{P}(y=2)} = o(1)$. See Figure 3 for an illustration of this data distribution. In this case, both e_1 and e_2 are features from the frequent classes 1 and 2. However, only e_1 helps classify the frequent classes and only e_2 can be transferred to the rare classes.

Algorithm formulations. For supervised learning, we train a two-layer linear network $f_{W_1, W_2}(x) \triangleq W_2 W_1 x$ with weight matrices $W_1 \in \mathbb{R}^{m \times d}$ and $W_2 \in \mathbb{R}^{3 \times m}$ for some $m \geq 3$, and then use the first layer $W_{\text{SL}} = W_1$ as the feature for downstream tasks. Given a linearly separable labeled dataset, we learn such a network with minimal norm $\|W_1^\top W_1\|_F^2 + \|W_2^\top W_2\|_F^2$ subject to the margin constraint $f_{W_1, W_2}(x)_y \geq f_{W_1, W_2}(x)_{y'} + 1$ for all data (x, y) in the dataset and $y' \neq y$.⁵ For self-supervised learned, similar to SimSiam [Chen et al., 2020], we construct positive pairs $(x + \xi, x + \xi')$ where x is from the empirical dataset, ξ and ξ' are independent random perturbations. We learn a matrix $W_{\text{SSL}} \in \mathbb{R}^{m \times d}$ which minimizes $-\hat{\mathbb{E}}[(W(x + \xi))^T (W(x + \xi'))] + \frac{1}{2} \|W^\top W\|_F^2$, where the expectation $\hat{\mathbb{E}}$ is over the empirical dataset and the randomness of ξ and ξ' . The regularization term $\frac{1}{2} \|W^\top W\|_F^2$ is introduced only to make the learned features more mathematically tractable. We use $W_{\text{SSL}} x$ as the feature of data x in the downstream task.

Main intuitions. We compare the features learned by SSL and supervised learning on an imbalanced dataset that contains an abundant (poly in d) number of data from the frequent classes but only a small (sublinear in d) number of data from the rare class. The key intuition behind our analysis is that supervised learning learns only the e_1 direction (which helps classify class 1 vs. class 2) and some random direction that overfits to the rare class. In contrast, self-supervised learning learns both e_1 and e_2 directions from the frequent classes. Since how well the feature helps classify the rare class (in ID evaluation) depends on how much it correlates with the e_2 direction, SSL provably learns features that help classify the rare class, while supervised learning fails. This intuition is formalized by the following theorem.

Theorem 3.1. *Let n_1, n_2, n_3 be the number of data from the three classes respectively. Let $\rho = d^{-\frac{1}{5}}$ and $\tau = d^{\frac{1}{5}}$ in the data generative model. For $n_1, n_2 = \Theta(\text{poly}(d))$ and $n_3 \leq d^{\frac{1}{5}}$, with probability at least $1 - O(e^{-d^{\frac{1}{10}}})$, the following statements hold for any feature dimension $m \geq 3$:*

- Let $W_{\text{SL}} = [w_1, w_2, \dots, w_m]^\top$ be the feature learned by SL, then $\sum_{i=1}^m \langle e_2, w_i \rangle^2 \leq O(d^{-\frac{1}{10}})$.

⁵Previous work shows that deep linear networks trained with gradient descent using logistic loss converge to this min norm solution in direction [Ji and Telgarsky, 2018].

- Let $W_{\text{SSL}} = [\tilde{w}_1, \tilde{w}_2, \dots, \tilde{w}_m]^\top$ be the feature learned by SSL, then $\|\Pi e_2\|_2 \geq 1 - O(d^{-\frac{1}{5}})$, where Π projects e_2 onto the row span of W_{SSL} .

Supervised learning results in features W_{SL} whose rows have small correlation with the transferable feature e_2 , indicating that supervised learning only learns features for classifying the frequent classes and ignore the transferable features. In contrast, self-supervised learning recovers e_2 well, even though e_2 is not relevant to classifying the frequent classes. The proofs are deferred to Section D. The analysis of supervised learning uses tools from the theory on max margin classifier, and particularly inspired by the lower bound technique in Wei et al. [2019]. The analysis of the self-supervised learning is somewhat inspired by HaoChen et al. [2021], but does not rely on it because the instances here are more structured.

3.2 Illustrative Semi-synthetic Experiments

In the previous subsection, we have shown that self-supervised learning provably learns label-irrelevant-but-transferable features from the frequent classes which can help classify the rare class in the toy case, while supervised learning mainly focuses on the label-relevant features. However, in real-world datasets, it is intractable to distinguish the two groups of features. To amplify this effect in a real-world dataset and highlight the insight of the theoretical analysis, we design a semi-synthetic experiment on SimCLR [Chen et al., 2020] to validate our conclusion.

Dataset. In the theoretical analysis above, the frequent classes contain both features related to the classification of frequent classes and features transferable to the the rare classes. Similarly, we consider an imbalanced pre-training dataset with two groups of features modified from CIFAR-10 as shown in Figure 4 (Left). We construct classes 1-5 as the frequent classes, where each class contains 5000 examples. Classes 6-10 are the rare classes, where each class has 10 examples. In this case, the ratio of imbalance $r = 0.002$. Each image from classes 1-5 consists of a left half and a right half. The left half of an example is from classes 1-5 of the original CIFAR-10 and corresponds to the label of that example. The right half is from a random image of CIFAR-10, which is label-irrelevant. In contrast, the left half of an example from classes 6-10 is blank, whereas the right half is label-relevant and from classes 6-10 of the original CIFAR-10. In this setting, features from the left halves of the images are correlated to the classification of the frequent classes, while features from the right halves are label-irrelevant for the frequent classes, but can help classify the rare classes. Note that features from the right halves cannot be directly learned from the rare classes since they have only 10 examples per class. This is consistent with the setting of Theorem 3.1.

Pre-training. We pre-train the representations on the semi-synthetic imbalanced dataset. For supervised learning, we use ResNet-50 on this 10-way classification task. For self-supervised learning, we use SimCLR with ResNet-50. To avoid confusing the left and right parts, we disable the random horizontal flip in the data augmentation. After pre-training, we fix the representations and train a linear classifier on top of the representations with balanced data from the 5 rare classes (25000 examples in total) to test if the model learns proper features for the rare classes during pre-training. In Figure 4 (Right), we test the classifier on the rare classes. In Figure 4 (Middle), we further visualize the Grad-CAM [Selvaraju et al., 2017] of the representations on the held-out set⁶.

Results. As a sanity check, we first pre-train a supervised model with only the 50 rare examples and train the linear head classifier with 25000 examples from the rare classes (5-way classification) to see if the model can learn proper features for the rare classes with only rare examples (Supervised-rare in Figure 4 (Right)). As expected, the accuracy is 36.5%, which is almost the same as randomly initialized representations with trained head classifier, indicating that the model cannot learn the features for the rare classes with only rare examples due to the limited number of examples. We then compare supervised learning with self-supervised learning on the whole semi-synthetic dataset. In Figure 4 (Right), self-supervised representations perform much better than supervised representations on the rare classes (70.1% vs 44.3%). We further visualize the activation maps of representations with Grad-CAM. Supervised learning mostly activate the left halves of the examples for both frequent and rare classes, indicating that it mainly learn features on the left. In sharp

⁶CIFAR images are of low resolution. For visualization, we use high resolution version of the CIFAR-10 images in Figure 4 (Middle). We also provide the visualization on original CIFAR-10 images in Figure 7.

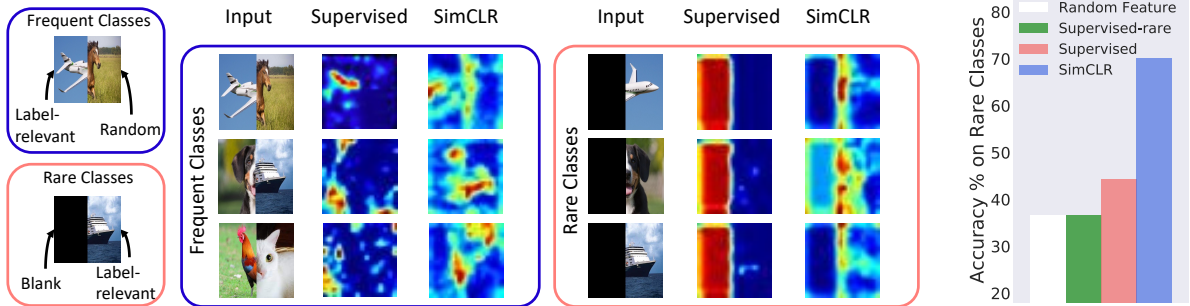


Figure 4: **Visualization of SSL’s features in semi-synthetic settings.** **Left:** The right halves of the rare examples decide the labels, while the left are blank. The left halves of the frequent examples decide the labels, while the right halves are random half images, which contain label-irrelevant-but-transferable features. **Middle:** Visualization of feature activations with Grad-CAM [Selvaraju et al., 2017]. SimCLR learns features from both left and right sides, whereas SL mainly learns label-relevant features from the left side of frequent data and ignore label-irrelevant features on the right side. **Right:** Accuracies evaluated on rare classes. The head linear classifiers are trained on 25000 examples from the 5 rare classes. Indeed, SimCLR learns much better features for rare classes than SL. Random Feature (feature extractor with randomly weights) and supervised-rare (features trained with only the rare examples) are included for references.

contrast, self-supervised learning activates the whole image on the frequent examples and the right part on the rare examples, indicating that it learns features from both parts.

4 Improving SSL on Imbalanced Datasets with Regularization

In this section, we aim to further improve the performance of SSL to close the gap between imbalanced and balanced datasets. Many prior works on imbalanced supervised learning regularize the rare classes more strongly, motivated by the observation that the rare classes suffer from more overfitting [Cao et al., 2019, 2021]. Inspired by these works, we compute the generalization gaps (i.e., the differences between empirical and validation pre-training losses) on frequent and rare classes for the step-imbalance CIFAR-10 datasets (where 5 classes are frequent class with 5000 examples per class and the rest are rare with 50 examples per class). Indeed, as shown in Table 1 (a), we still observe a similar phenomenon—the frequent classes have much smaller pre-training generalization gap than the rare classes (0.035 vs. 0.081), which indicates the necessity of more regularization on the rare classes.

We need a data-dependent regularizer that can have different effects on rare and frequent examples. Thus, weight decay or dropout [Srivastava et al., 2014] are not suitable. The prior work of Cao et al. [2019] regularizes the rare classes more strongly with larger margin, but it does not apply to SSL where no labels are available. Inspired by Cao et al. [2021], we adapt sharpness-aware minimization (SAM) [Foret et al., 2021] to imbalanced SSL.

Reweighted SAM (rwSAM). SAM improves model generalization by penalizing loss sharpness. Suppose the training loss of the representation f_ϕ is $\widehat{L}(\phi)$, i.e. $\widehat{L}(\phi) = \frac{1}{n} \sum_{j=1}^n \ell(x_j, \phi)$. SAM seeks parameters where the loss is uniformly low in the neighboring area,

$$\min_{\phi} \widehat{L}(\phi + \epsilon(\phi)), \quad \text{where} \quad \epsilon(\phi) = \arg \max_{\|\epsilon\| < \rho} \epsilon^\top \nabla_{\phi} \widehat{L}(\phi). \quad (2)$$

To take the weight of different examples into account, we add reweighting to the inner maximization step of SAM. Intuitively, we wish the optimization landscape to be flatter for rare examples, which is in effect regularizing the model more on rare examples. Concretely, consider the reweighted training loss associated with weight vector $w \in \mathbb{R}^n$, $\widehat{L}_w(\phi) = \frac{1}{n} \sum_{j=1}^n w_j \ell(x_j, \phi)$. The reweighted SAM objective re-weights the

(a) CIFAR, ID		$r = 0.01, \text{ step}$			$r = 0.01, \text{ exp}$	
Method	Acc. (%)	Gap Freq.	Gap Rare	Acc. (%)		
SimSiam	84.3 ± 0.2	0.035	0.081	81.4 ± 0.3		
SimSiam+SAM	84.7 ± 0.3	0.044	0.075	82.1 ± 0.4		
SimSiam, balanced	85.8 ± 0.2	0.038	0.037	82.0 ± 0.4		
SimSiam+rwSAM	85.6 ± 0.4	0.037	0.066	82.7 ± 0.5		
(b) ImageNet, OOD		Target dataset				
Method	CUB	Cars	Aircrafts	Pets	Avg.	
MoCo v2	69.9 ± 0.7	88.4 ± 0.4	82.9 ± 0.6	80.1 ± 0.6	80.3	
MoCo v2+SAM	69.9 ± 0.5	88.8 ± 0.5	83.4 ± 0.4	81.5 ± 0.8	80.9	
MoCo v2, balanced	69.8 ± 0.5	88.6 ± 0.4	82.7 ± 0.5	80.0 ± 0.4	80.2	
MoCo v2+rwSAM	70.3 ± 0.7	88.7 ± 0.3	84.9 ± 0.6	81.7 ± 0.4	81.4	
SimSiam	70.0 ± 0.3	87.0 ± 0.6	81.5 ± 0.7	83.8 ± 0.5	80.6	
SimSiam, balanced	70.5 ± 0.8	87.9 ± 0.7	81.8 ± 0.7	82.7 ± 0.4	80.7	
SimSiam+rwSAM	70.7 ± 0.8	88.4 ± 0.6	82.6 ± 0.6	84.0 ± 0.4	81.4	

Table 1: **Results of the proposed rwSAM.** (a) Results on CIFAR-10-LT with linear probe and ID evaluation. SimSiam+rwSAM on imbalanced datasets performs even better than SimSiam on balanced datasets with the same number of examples. Note that rwSAM closes the generalization gap on the rare examples (0.081 vs. 0.066). (b) Results on ImageNet-LT with fine-tuning and OOD evaluation. rwSAM improves the performance of MoCo v2 and SimSiam on the target datasets.

regularization-related terms (e.g., ϵ_w) but not the training loss \widehat{L} :

$$\min_{\phi} \widehat{L}(\phi + \epsilon_w(\phi)), \quad \text{where} \quad \epsilon_w(\phi) = \arg \max_{\|\epsilon\| < \rho} \epsilon^\top \nabla_{\phi} \widehat{L}_w(\phi). \quad (3)$$

Assigning Weight with Kernel Density Estimation. The weight w_j of an example x_j should be inversely correlated with the frequency of the corresponding class y_j . However, we have no access to the labels. In order to approximate the frequency of examples, we use kernel density estimation on top of the representations f_{ϕ} . Concretely, denote by $K(\cdot, h)$ the Gaussian density with bandwidth h . We assign w_i to be inversely correlated with the estimated density, i.e., $w_i = \left(\frac{1}{n} \sum_{j=1}^n K(f_{\phi}(x_i) - f_{\phi}(x_j), h)\right)^{-\alpha}$ where h and $\alpha > 0$ are hyperparameters selected by cross validation.

4.1 Experiments

We test the proposed rwSAM on CIFAR-10 with step or exponential imbalance and ImageNet-LT [Liu et al., 2019]. After self-supervised pre-training on the long-tailed dataset, we evaluate the representations by (1) linear probing on the balanced in-domain dataset and (2) fine-tuning on downstream target datasets. For (1) and (2), we compare with SSL, SSL+SAM (w/o reweighting), and SSL balanced, which learns the representations on the balanced dataset *with the same number of examples*. Implementation details and additional results are deferred to Section C. Code is available at <https://github.com/Liuhong99/Imbalanced-SSL>.

Results. Table 1 (a) summarizes results on long tailed CIFAR-10. With both step and exponential imbalance, rwSAM improves the performance of SimSiam over 1%, and even surpasses the performance of SimSiam on balanced CIFAR-10 with the same number of examples. Note that compared to SimSiam, rwSAM closes the generalization gap of pre-training loss on rare examples from 0.081 to 0.066, which verifies the effect of re-weighted regularization. In Table 1 (b), we provide the result of fine-tuning on downstream tasks with representations pre-trained on ImageNet-LT. The proposed method improves the transferability of representations to downstream tasks consistently.

5 Related Work

5.1 Supervised Learning with Dataset Imbalance

There exists a long line of works studying supervised imbalanced classification [He and Garcia, 2009, Krawczyk, 2016]. Early works on ensemble learning adjusted the boosting and bagging algorithms with resampling in the imbalanced setting [Guo and Viktor, 2004, Wang and Yao, 2009]. Classical methods include resampling and reweighting. Hart [1968], Kubat et al. [1997], Chawla et al. [2002], He et al. [2008], Ando and Huang [2017], Buda et al. [2018], Hu et al. [2020] proposed to re-sample the data to make the frequent and rare classes appear with equal frequency in training. Re-weighting assigns different weights for head and tail classes and eases the optimization difficulty under class imbalance [Cui et al., 2019, Tang et al., 2020, Wang et al., 2017b, Huang et al., 2019]. Byrd and Lipton [2019] empirically studied the effect of importance weighting and found out that importance weighting does not change the solution without regularization. Xu et al. [2021] justified this finding with theoretical analysis based on the implicit bias of gradient descent on separable data.

Cao et al. [2019] initiated the idea of using re-weighted regularization and proposed the principle of regularizing rare classes more heavily. Re-weighted regularization is shown to be typically more effective than re-weighting or re-sampling the losses. Cao et al. [2021] proposed to regularize the local curvature of loss on imbalanced and noisy datasets.

Works in the modern deep learning era also designed specific losses or training pipelines for imbalanced recognition [Tang et al., 2020, Hong et al., 2021, Wang et al., 2021, Zhang et al., 2021]. Lin et al. [2017] proposed to focus on hard examples to prevent easy examples from overwhelming the models during training. Meta-learning approaches meta-learned the weight or the ensemble [Wang et al., 2017b, Ren et al., 2018, Shu et al., 2019, Lee et al., 2020a]. Liu et al. [2019], Jamal et al. [2020], Liu et al. [2020] improved the performance on the rare examples by explicitly encouraging transfer learning. Re-calibration methods adjust the logits of the outputs with re-weighting [Tian et al., 2020, Menon et al., 2021].

Several works also studied the supervised representations under dataset imbalance. Kang et al. [2020], Wang et al. [2020] found out that the representations of supervised learning perform better than the classifier itself with class imbalance. Yang and Xu [2020] studied the effect of self-training and self-supervised pre-training on supervised imbalanced recognition classifiers. In contrast, the focus of our paper is the effect of class imbalance on *self-supervised representations*.

5.2 Self-supervised Learning

Earlier works on self-supervised learning learned visual representations by context prediction [Doersch et al., 2015, Wang et al., 2017a], solving puzzles [Noroozi and Favaro, 2016], and rotation prediction [Gidaris et al., 2018]. Recent works on self-supervised learning successfully learn representations that approach the supervised baseline on ImageNet and various downstream tasks, and closed the gap with supervised pre-training. Contrastive learning methods attract positive pairs and drive apart negative pairs [He et al., 2020, Chen et al., 2020]. Siamese networks predict the output of the other branch, and use stop-gradient to avoid collapsing [Grill et al., 2020, Chen and He, 2021]. Clustering methods learn representations by performing clustering on the representations and improve the representations with cluster index [Caron et al., 2020]. Cole et al. [2021] investigated the effect of data quantity and task granularity on self-supervised representations. Goyal et al. [2021] studied self-supervised methods on large scale datasets in the wild, but they do not consider dataset imbalance explicitly. Kotar et al. [2021] studied whether dataset imbalance can have a significant impact on contrastive learning representations. Madaan et al. [2022] found out that self-supervised representations are better at continual learning than supervised representations. Several works have also theoretically studied the success of self-supervised learning [Arora et al., 2019, HaoChen et al., 2021, Wei et al., 2021, Lee et al., 2020b, Tian et al., 2021, Tosh et al., 2020, 2021]. Our analysis in Section 3.1 is partially inspired by the work HaoChen et al. [2020].

6 Conclusion

Our paper is the first to study the problem of robustness to imbalanced training of self-supervised representations. We discover that self-supervised representations are more robust to class imbalance than supervised representations and explore the underlying cause of this phenomenon. As supervised learning is still the de facto standard for pre-training, our work should encourage practitioners to use SSL for pre-training instead, or at least consider evaluating the impact of imbalanced pre-training on their downstream task. Our experiments mainly focus on vision datasets. Future works can study the effect of dataset imbalance on NLP datasets, where self-supervised pre-training is a dominant approach. We hope our study can inspire analysis of self-supervised learning in broader environments in the wild such as domain shift, and provide insights for the design of future unsupervised learning methods.

Acknowledgements

We thank Colin Wei, Margalit Glasgow, and Shibani Santurkar for helpful discussions. TM acknowledges support of Google Faculty Award, NSF IIS 2045685, the Sloan Fellowship, and JD.com. Toyota Research Institute provided funds to support this work.

References

- Shin Ando and Chun Yuan Huang. Deep over-sampling framework for classifying imbalanced data. In *Joint European Conference on Machine Learning and Knowledge Discovery in Databases*, pages 770–785, 2017.
- Sanjeev Arora, Hrishikesh Khandeparkar, Mikhail Khodak, Orestis Plevrakis, and Nikunj Saunshi. A theoretical analysis of contrastive unsupervised representation learning. In *International Conference on Machine Learning*, 2019.
- Mateusz Buda, Atsuto Maki, and Maciej A Mazurowski. A systematic study of the class imbalance problem in convolutional neural networks. *Neural Networks*, 106:249–259, 2018.
- Jonathon Byrd and Zachary Lipton. What is the effect of importance weighting in deep learning? In *International Conference on Machine Learning*, pages 872–881. PMLR, 2019.
- Kaidi Cao, Colin Wei, Adrien Gaidon, Nikos Arechiga, and Tengyu Ma. Learning imbalanced datasets with label-distribution-aware margin loss. In *Advances in Neural Information Processing Systems*, volume 32, pages 1565–1576. Curran Associates, Inc., June 2019.
- Kaidi Cao, Yining Chen, Junwei Lu, Nikos Arechiga, Adrien Gaidon, and Tengyu Ma. Heteroskedastic and imbalanced deep learning with adaptive regularization. In *International Conference on Learning Representations*, 2021.
- Mathilde Caron, Ishan Misra, Julien Mairal, Priya Goyal, Piotr Bojanowski, and Armand Joulin. Unsupervised learning of visual features by contrasting cluster assignments. *arXiv preprint arXiv:2006.09882*, 33:9912–9924, 2020.
- Nitesh V Chawla, Kevin W Bowyer, Lawrence O Hall, and W Philip Kegelmeyer. Smote: synthetic minority over-sampling technique. *Journal of artificial intelligence research*, 16:321–357, 2002.
- Ting Chen, Simon Kornblith, Mohammad Norouzi, and Geoffrey Hinton. A simple framework for contrastive learning of visual representations. In *International conference on machine learning*, volume 119 of *Proceedings of Machine Learning Research*, pages 1597–1607. PMLR, PMLR, 13–18 Jul 2020.

- Xinlei Chen and Kaiming He. Exploring simple siamese representation learning. In *Proceedings of the IEEE/CVF Conference on Computer Vision and Pattern Recognition (CVPR)*, pages 15750–15758, June 2021.
- Adam Coates, Andrew Y Ng, and Honglak Lee. An analysis of single-layer networks in unsupervised feature learning. In *International Conference on Artificial Intelligence and Statistics*, pages 215–223, 2011.
- Elijah Cole, Xuan Yang, Kimberly Wilber, Oisín Mac Aodha, and Serge Belongie. When does contrastive visual representation learning work? *arXiv preprint arXiv:2105.05837*, 2021.
- Ekin D Cubuk, Barret Zoph, Jonathon Shlens, and Quoc V Le. Randaugment: Practical automated data augmentation with a reduced search space. In *Proceedings of the IEEE/CVF Conference on Computer Vision and Pattern Recognition Workshops*, pages 702–703, 2020.
- Yin Cui, Menglin Jia, Tsung-Yi Lin, Yang Song, and Serge Belongie. Class-balanced loss based on effective number of samples. In *Proceedings of the IEEE/CVF conference on computer vision and pattern recognition*, pages 9268–9277, 2019.
- Carl Doersch, Abhinav Gupta, and Alexei A Efros. Unsupervised visual representation learning by context prediction. In *Proceedings of the IEEE international conference on computer vision*, pages 1422–1430, 2015.
- Pierre Foret, Ariel Kleiner, Hossein Mobahi, and Behnam Neyshabur. Sharpness-aware minimization for efficiently improving generalization. *arXiv preprint arXiv:2010.01412*, 2020.
- Pierre Foret, Ariel Kleiner, Hossein Mobahi, and Behnam Neyshabur. Sharpness-aware minimization for efficiently improving generalization. In *International Conference on Learning Representations*, 2021.
- Spyros Gidaris, Praveer Singh, and Nikos Komodakis. Unsupervised representation learning by predicting image rotations. *arXiv preprint arXiv:1803.07728*, 2018.
- Priya Goyal, Mathilde Caron, Benjamin Lefaudeux, Min Xu, Pengchao Wang, Vivek Pai, Mannat Singh, Vitaliy Liptchinsky, Ishan Misra, Armand Joulin, et al. Self-supervised pretraining of visual features in the wild. *arXiv preprint arXiv:2103.01988*, 2021.
- Jean-Bastien Grill, Florian Strub, Florent Altché, Corentin Tallec, Pierre H Richemond, Elena Buchatskaya, Carl Doersch, Bernardo Avila Pires, Zhaohan Daniel Guo, Mohammad Gheshlaghi Azar, et al. Bootstrap your own latent: A new approach to self-supervised learning. *arXiv preprint arXiv:2006.07733*, 33: 21271–21284, 2020.
- Hongyu Guo and Herna L Viktor. Learning from imbalanced data sets with boosting and data generation: the databoost-im approach. *ACM Sigkdd Explorations Newsletter*, 6(1):30–39, 2004.
- Jeff Z HaoChen, Colin Wei, Jason D Lee, and Tengyu Ma. Shape matters: Understanding the implicit bias of the noise covariance. *arXiv preprint arXiv:2006.08680*, 2020.
- Jeff Z HaoChen, Colin Wei, Adrien Gaidon, and Tengyu Ma. Provable guarantees for self-supervised deep learning with spectral contrastive loss. *arXiv preprint arXiv:2106.04156*, 2021.
- Peter Hart. The condensed nearest neighbor rule (corresp.). *IEEE transactions on information theory*, 14(3): 515–516, 1968.
- Haibo He and Edwardo A Garcia. Learning from imbalanced data. *IEEE Transactions on knowledge and data engineering*, 21(9):1263–1284, 2009.
- Haibo He, Yang Bai, Edwardo A Garcia, and Shutao Li. Adasyn: Adaptive synthetic sampling approach for imbalanced learning. In *2008 IEEE international joint conference on neural networks (IEEE world congress on computational intelligence)*, pages 1322–1328. IEEE, 2008.

- Kaiming He, Xiangyu Zhang, Shaoqing Ren, and Jian Sun. Deep residual learning for image recognition. In *Proceedings of the IEEE conference on computer vision and pattern recognition*, pages 770–778, 2016.
- Kaiming He, Haoqi Fan, Yuxin Wu, Saining Xie, and Ross Girshick. Momentum contrast for unsupervised visual representation learning. In *Proceedings of the IEEE/CVF Conference on Computer Vision and Pattern Recognition*, pages 9729–9738, June 2020.
- Youngkyu Hong, Seungju Han, Kwanghee Choi, Seokjun Seo, Beomsu Kim, and Buru Chang. Disentangling label distribution for long-tailed visual recognition. In *Proceedings of the IEEE/CVF Conference on Computer Vision and Pattern Recognition*, pages 6626–6636, 2021.
- Xinting Hu, Yi Jiang, Kaihua Tang, Jingyuan Chen, Chunyan Miao, and Hanwang Zhang. Learning to segment the tail. In *Proceedings of the IEEE/CVF Conference on Computer Vision and Pattern Recognition*, pages 14045–14054, 2020.
- Chen Huang, Yining Li, Chen Change Loy, and Xiaoou Tang. Deep imbalanced learning for face recognition and attribute prediction. *IEEE transactions on pattern analysis and machine intelligence*, 42(11):2781–2794, 2019.
- Muhammad Abdullah Jamal, Matthew Brown, Ming-Hsuan Yang, Liqiang Wang, and Boqing Gong. Rethinking class-balanced methods for long-tailed visual recognition from a domain adaptation perspective. In *Proceedings of the IEEE/CVF Conference on Computer Vision and Pattern Recognition (CVPR)*, June 2020.
- Ziwei Ji and Matus Telgarsky. Gradient descent aligns the layers of deep linear networks. *arXiv preprint arXiv:1810.02032*, 2018.
- Bingyi Kang, Saining Xie, Marcus Rohrbach, Zhicheng Yan, Albert Gordo, Jiashi Feng, and Yannis Kalantidis. Decoupling representation and classifier for long-tailed recognition. In *International Conference on Learning Representations*, 2020.
- Klemen Kotar, Gabriel Ilharco, Ludwig Schmidt, Kiana Ehsani, and Roozbeh Mottaghi. Contrasting contrastive self-supervised representation learning pipelines. In *Proceedings of the IEEE/CVF International Conference on Computer Vision*, pages 9949–9959, 2021.
- Jonathan Krause, Michael Stark, Jia Deng, and Li Fei-Fei. 3d object representations for fine-grained categorization. In *Proceedings of the IEEE international conference on computer vision workshops*, pages 554–561, 2013.
- Bartosz Krawczyk. Learning from imbalanced data: open challenges and future directions. *Progress in Artificial Intelligence*, 5(4):221–232, 2016.
- Alex Krizhevsky and Geoffrey Hinton. Learning multiple layers of features from tiny images. 2009.
- Miroslav Kubat, Stan Matwin, et al. Addressing the curse of imbalanced training sets: one-sided selection. In *Icml*, volume 97, pages 179–186. Citeseer, 1997.
- Hae Beom Lee, Hayeon Lee, Donghyun Na, Saehoon Kim, Minseop Park, Eunho Yang, and Sung Ju Hwang. Learning to balance: Bayesian meta-learning for imbalanced and out-of-distribution tasks. In *International Conference on Learning Representations*, 2020a.
- Jason D Lee, Qi Lei, Nikunj Saunshi, and Jiacheng Zhuo. Predicting what you already know helps: Provable self-supervised learning. *arXiv preprint arXiv:2008.01064*, 2020b.
- Tsung-Yi Lin, Priya Goyal, Ross Girshick, Kaiming He, and Piotr Dollár. Focal loss for dense object detection. In *Proceedings of the IEEE international conference on computer vision*, pages 2980–2988, 2017.

- Jialun Liu, Yifan Sun, Chuchu Han, Zhaopeng Dou, and Wenhui Li. Deep representation learning on long-tailed data: A learnable embedding augmentation perspective. In *Proceedings of the IEEE/CVF Conference on Computer Vision and Pattern Recognition*, pages 2970–2979, 2020.
- Ziwei Liu, Zhongqi Miao, Xiaohang Zhan, Jiayun Wang, Boqing Gong, and Stella X. Yu. Large-scale long-tailed recognition in an open world. In *Proceedings of the IEEE/CVF Conference on Computer Vision and Pattern Recognition (CVPR)*, June 2019.
- Divyam Madaan, Jaehong Yoon, Yuanchun Li, Yunxin Liu, and Sung Ju Hwang. Representational continuity for unsupervised continual learning. In *International Conference on Learning Representations*, 2022.
- Subhansu Maji, Esa Rahtu, Juho Kannala, Matthew Blaschko, and Andrea Vedaldi. Fine-grained visual classification of aircraft. *arXiv preprint arXiv:1306.5151*, 2013.
- Aditya Krishna Menon, Sadeep Jayasumana, Ankit Singh Rawat, Himanshu Jain, Andreas Veit, and Sanjiv Kumar. Long-tail learning via logit adjustment. In *International Conference on Learning Representations*, 2021.
- Mehdi Noroozi and Paolo Favaro. Unsupervised learning of visual representations by solving jigsaw puzzles. In *European conference on computer vision*, pages 69–84. Springer, 2016.
- Omkar M Parkhi, Andrea Vedaldi, Andrew Zisserman, and CV Jawahar. Cats and dogs. In *2012 IEEE conference on computer vision and pattern recognition*, pages 3498–3505, 2012.
- William J Reed. The pareto, zipf and other power laws. *Economics letters*, 74(1):15–19, 2001.
- Mengye Ren, Wenyuan Zeng, Bin Yang, and Raquel Urtasun. Learning to reweight examples for robust deep learning. In *International Conference on Machine Learning*, pages 4334–4343, 2018.
- Olga Russakovsky, Jia Deng, Hao Su, Jonathan Krause, Sanjeev Satheesh, Sean Ma, Zhiheng Huang, Andrej Karpathy, Aditya Khosla, Michael Bernstein, Alexander C. Berg, and Li Fei-Fei. ImageNet Large Scale Visual Recognition Challenge. *International Journal of Computer Vision*, 115(3):211–252, 2015.
- Ramprasaath R Selvaraju, Michael Cogswell, Abhishek Das, Ramakrishna Vedantam, Devi Parikh, and Dhruv Batra. Grad-cam: Visual explanations from deep networks via gradient-based localization. In *Proceedings of the IEEE international conference on computer vision*, pages 618–626, 2017.
- Jun Shu, Qi Xie, Lixuan Yi, Qian Zhao, Sanping Zhou, Zongben Xu, and Deyu Meng. Meta-weight-net: Learning an explicit mapping for sample weighting. In *Advances in Neural Information Processing Systems*, volume 32. Curran Associates, Inc., 2019.
- Nitish Srivastava, Geoffrey Hinton, Alex Krizhevsky, Ilya Sutskever, and Ruslan Salakhutdinov. Dropout: a simple way to prevent neural networks from overfitting. *The journal of machine learning research*, 15(1): 1929–1958, 2014.
- Kaihua Tang, Jianqiang Huang, and Hanwang Zhang. Long-tailed classification by keeping the good and removing the bad momentum causal effect. In *Advances in Neural Information Processing Systems*, volume 33, pages 1513–1524. Curran Associates, Inc., 2020.
- Junjiao Tian, Yen-Cheng Liu, Nathan Glaser, Yen-Chang Hsu, and Zsolt Kira. Posterior re-calibration for imbalanced datasets. *arXiv preprint arXiv:2010.11820*, 2020.
- Yuandong Tian, Xinlei Chen, and Surya Ganguli. Understanding self-supervised learning dynamics without contrastive pairs. *arXiv preprint arXiv:2102.06810*, 2021.
- Christopher Tosh, Akshay Krishnamurthy, and Daniel Hsu. Contrastive estimation reveals topic posterior information to linear models. *arXiv:2003.02234*, 2020.

- Christopher Tosh, Akshay Krishnamurthy, and Daniel Hsu. Contrastive learning, multi-view redundancy, and linear models. In *Algorithmic Learning Theory*, pages 1179–1206. PMLR, 2021.
- Roman Vershynin. *High-dimensional probability: An introduction with applications in data science*, volume 47. Cambridge university press, 2018.
- Catherine Wah, Steve Branson, Peter Welinder, Pietro Perona, and Serge Belongie. The caltech-ucsd birds-200-2011 dataset. 2011.
- Shuo Wang and Xin Yao. Diversity analysis on imbalanced data sets by using ensemble models. In *2009 IEEE symposium on computational intelligence and data mining*, pages 324–331. IEEE, 2009.
- Tao Wang, Yu Li, Bingyi Kang, Junnan Li, Junhao Liew, Sheng Tang, Steven Hoi, and Jiashi Feng. The devil is in classification: A simple framework for long-tail instance segmentation. In *European Conference on computer vision*, pages 728–744. Springer, 2020.
- Xiaolong Wang, Kaiming He, and Abhinav Gupta. Transitive invariance for self-supervised visual representation learning. In *Proceedings of the IEEE international conference on computer vision*, pages 1329–1338, 2017a.
- Xudong Wang, Long Lian, Zhongqi Miao, Ziwei Liu, and Stella Yu. Long-tailed recognition by routing diverse distribution-aware experts. In *International Conference on Learning Representations*, 2021.
- Yu-Xiong Wang, Deva Ramanan, and Martial Hebert. Learning to model the tail. In *Proceedings of the 31st International Conference on Neural Information Processing Systems*, pages 7032–7042, 2017b.
- Colin Wei, Jason D Lee, Qiang Liu, and Tengyu Ma. Regularization matters: Generalization and optimization of neural nets vs their induced kernel. In *Advances in Neural Information Processing Systems*, pages 9709–9721, 2019.
- Colin Wei, Sang Michael Xie, and Tengyu Ma. Why do pretrained language models help in downstream tasks? an analysis of head and prompt tuning. *arXiv preprint arXiv:2106.09226*, 2021.
- Da Xu, Yuting Ye, and Chuanwei Ruan. Understanding the role of importance weighting for deep learning. In *International Conference on Learning Representations*, 2021.
- Yuzhe Yang and Zhi Xu. Rethinking the value of labels for improving class-imbalanced learning. In *Advances in Neural Information Processing Systems*, volume 33, pages 19290–19301. Curran Associates, Inc., 2020.
- Yuzhe Yang, Kaiwen Zha, Yingcong Chen, Hao Wang, and Dina Katabi. Delving into deep imbalanced regression. In *Proceedings of the 38th International Conference on Machine Learning*, volume 139 of *Proceedings of Machine Learning Research*, pages 11842–11851, 18–24 Jul 2021.
- Songyang Zhang, Zeming Li, Shipeng Yan, Xuming He, and Jian Sun. Distribution alignment: A unified framework for long-tail visual recognition. In *Proceedings of the IEEE/CVF Conference on Computer Vision and Pattern Recognition*, pages 2361–2370, 2021.

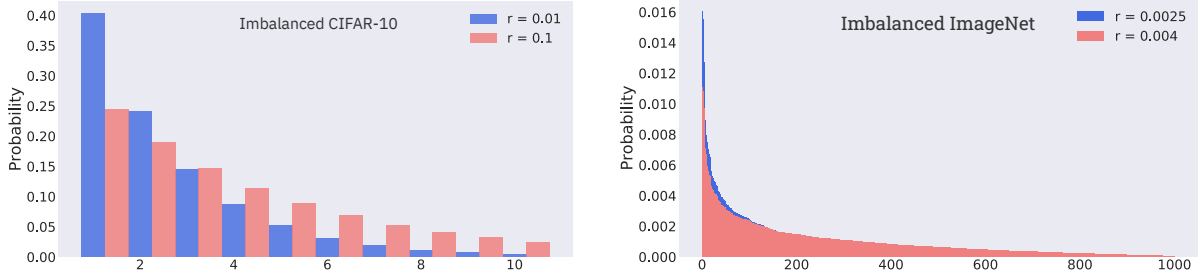


Figure 5: **Visualization of the label distributions.** We visualize the label distributions of the imbalanced CIFAR-10 and ImageNet. We consider two imbalance ratios r for each dataset. Imbalanced CIFAR-10 follows the exponential distribution, while imbalanced ImageNet follows Pareto distribution.

A Details of Section 2

A.1 Implementation Details

Generating Pre-training Datasets. CIFAR-10 [Krizhevsky and Hinton, 2009] contains 10 classes with 5000 examples per class. We use exponential imbalance, i.e. for class c , the number of examples is $5000 \times e^{\beta(c-1)}$. we consider imbalance ratio $r \in \{0.1, 0.01\}$, i.e. the number of examples belonging to the rarest class is 500 or 50. The total n_s is therefore 20431 or 12406. ImageNet-LT is constructed by Liu et al. [2019], which follows the Pareto distribution with the power value 6. The number of examples from the rarest class is 5. We construct a long tailed ImageNet following the Pareto distribution with more imbalance, where the number of examples from the rarest class is 3. The total number of examples n_s is 115846 and 80218 respectively. For each ratio of imbalance, we further downsample the dataset with the sampling ratio in $\{0.75, 0.5, 0.25, 0.125\}$ to formulate different number of examples. To compare with the balanced setting fairly, we also sample balanced versions of datasets with the same number of examples. Note that each variant of the dataset is fixed after construction for all algorithms. See the visualization of label distributions of dataset variants in Figure 5.

Training Procedure. For supervised pre-training, we follow the standard protocol of He et al. [2016] and Kang et al. [2020]. On the standard ImageNet-LT, we train the models for 90 epochs with step learning rate decay. For down-sampled variants, the training epochs are selected with cross validation. For self-supervised learning, the initial learning rate on the standard ImageNet-LT is set to 0.025 with batch-size 256. We train the model for 300 epochs on the standard ImageNet-LT and adopt cosine learning rate decay following [He et al., 2020, Chen and He, 2021]. We train the models for more epochs on the down sampled variants to ensure the same number of total iterations. The code on CIFAR-10 LT is adapted from <https://github.com/Reza-Safdari/SimSiam-91.9-top1-acc-on-CIFAR10>.

Evaluation. For in-domain evaluation (ID), we first train the the representations on the aforementioned dataset variants, and then train the linear head classifier on the *full balanced* CIFAR10 or ImageNet. We set the initial learning rate to 30 when training the linear head with batch-size 4096 and train for 100 epochs in total. For in-domain out-of-domain evaluation (OOD) on ImageNet, we first train the the representations on the aforementioned dataset variants, and then fine-tune the model to CUB-200 [Wah et al., 2011], Stanford Cars [Krause et al., 2013], Oxford Pets [Parkhi et al., 2012], and Aircrafts [Maji et al., 2013]. The number of examples of these target datasets ranges from 2k to 10k, which is a reasonable scale as the number of examples of the pre-training dataset variants ranges from 10k to 110k. The representation quality is evaluated with the average performance on the four tasks. We set the initial learning rate to 0.1 in fine-tuning train for 150 epochs in total. For in-domain out-of-domain evaluation (OOD) on CIFAR-10, we use STL-10 as the downstream target tasks and perform linear probe.

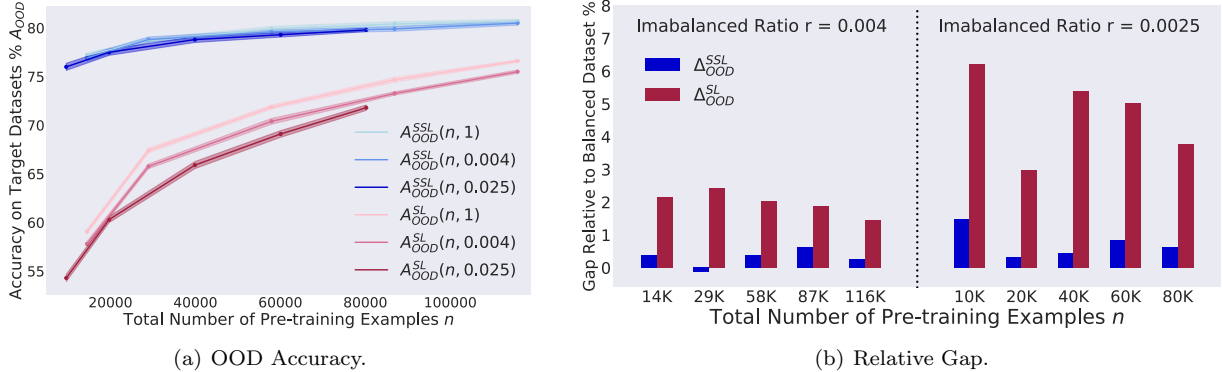


Figure 6: **OOD Results of SimSiam on ImageNet.** SimSiam also demonstrates more robustness to class imbalance compared to supervised learning. The relative gap to balanced dataset is much smaller than supervised learning across different imbalance ratios.

Table 2: Numbers in Figure 2 and Figure 6.

Imbalanced Ratio r	$r = 1$, balanced					$r = 0.004$					$r = 0.0025$				
Data Quantity n	116K	87K	58K	29K	14K	116K	87K	58K	29K	14K	80K	60K	40K	20K	10K
MoCo V2, ID	50.4	43.5	40.9	37.0	30.8	49.5	43.2	39.5	36.6	30.5	40.6	38.8	35.5	31.9	27.2
MoCo V2, OOD	80.3	79.8	79.7	77.4	77.0	80.2	80.1	79.5	77.8	77.3	79.2	78.8	77.7	75.6	74.4
Supervised, ID	54.3	51.6	46.1	40.5	26.3	52.9	49.6	44.0	37.3	24.9	46.1	42.0	36.3	27.5	20.3
Supervised, OOD	76.6	74.7	71.9	67.4	59.1	75.5	73.3	70.4	65.8	57.8	71.8	69.1	65.9	60.3	54.3
SimSiam, OOD	80.7	80.4	79.9	78.7	77.2	80.6	79.9	79.6	78.8	76.9	79.8	79.3	78.8	77.5	76.0

A.2 Additional Results

To validate the phenomenon observed in Section 2 is consistent for different self-supervised learning algorithms, we provide the OOD evaluation results of SimSiam trained on ImageNet variants and relative performance gap with balanced datasets in Figure 6. SimSiam representations are also less sensitive to class imbalance than supervised representations.

We also provide the numbers of Figure 2 and Figure 6 in Table 2.

B Details of Section 3.2

We first generate the balanced semi-synthetic dataset with 5000 examples per class. The left halves of images from classes 1-5 correspond to the labels, while the right halves are random. The left halves of images from class 6-10 are blank, whereas the right halves correspond to the labels. We then generate the imbalanced dataset, which consists of the 5000 examples per class from classes 1-5 (frequent classes), and 10 examples per class from classes 6-10 (rare classes). We use Grad-CAM implementation based on <https://github.com/meliketoy/gradcam.pytorch> and SimCLR implementation from <https://github.com/leftthomas/SimCLR>. We provide examples and Grad-CAM of the semi-synthetic datasets in Figure 7.

C Details of Section 4

C.1 Implementation Details

We use the same implementation as Section 2 for supervised and self-supervised learning baselines. We implement sharpness-aware minimization following [Foret et al., 2021]. In each step of update, we first

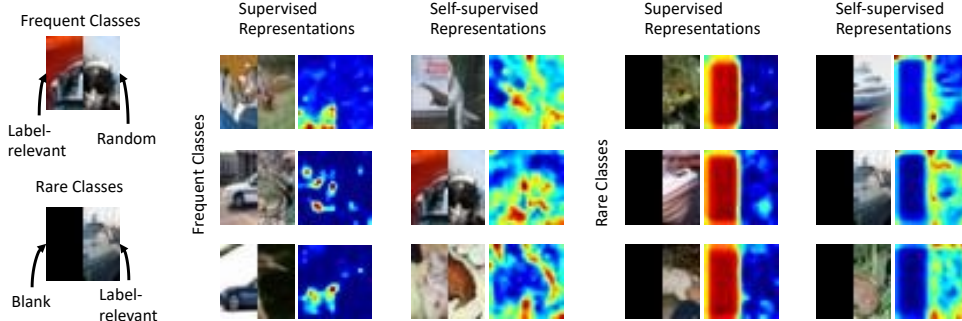


Figure 7: **Examples of the semi-synthetic Datasets and Grad-CAM visualizations.** SimCLR learns features from both left and right sides, whereas SL mainly learns label-relevant features from the left side of frequent data and ignore label-irrelevant features on the right side. In Figure 4, we provide results the high-resolution images of the 10 CIFAR classes to make the results easier to interpret. Here we further visualize the results on original CIFAR-10 images.

compute the reweighted loss $\widehat{L}_w(\phi) = \frac{1}{n} \sum_{j=1}^n w_j \ell(x_j, \phi)$ and compute its gradient w.r.t. ϕ , i.e. $\nabla_{\phi} \widehat{L}_w(\phi)$. Then we can compute $\epsilon(\phi)$ as $\epsilon(\phi) = \rho \text{sgn}(\nabla_{\phi} \widehat{L}_w(\phi)) \left| \nabla_{\phi} \widehat{L}_w(\phi) \right|^{q-1} / \left(\|\nabla_{\phi} \widehat{L}_w(\phi)\|_q^q \right)^{1/p}$, where $\frac{1}{p} + \frac{1}{q} = 1$. Finally, we update the model on the loss without reweighting $\widehat{L}(\phi)$ by $\phi = \phi - \eta \nabla_{\phi} \widehat{L}(\phi + \epsilon(\phi))$. A detailed algorithm can be viewed in Algorithm 1.

We select the hyperparameters ρ and α with cross validation. On ImageNet-LT and iNaturalist, $\rho = 2$ and $\alpha = 0.5$. On CIFAR-10-LT, $\rho = 5$ and $\alpha = 1.2$.

C.2 Additional Results

We further introduce another evaluation protocol of the representations learned on imbalanced ImageNet: following the protocol of Kang et al. [2020], Yang and Xu [2020], we fine-tune the representations on *imbalanced* ImageNet dataset with supervision, and then re-train the linear classifier with *class-aware resampling*, to compare with supervised imbalanced recognition methods. In MoCo V2 pre-training, we use the standard data augmentation following He et al. [2020]. In fine-tuning, we use RandAugment [Cubuk et al., 2020]. For this evaluation, we further compare with CRT [Kang et al., 2020], LADE [Hong et al., 2021], and RIDE [Wang et al., 2021], which are strong methods tailored to supervised imbalanced recognition. Results are provided in Table 3. Supervised here refers to training the feature extractor and linear classifier with supervision on the imbalanced dataset directly. CRT first trains the feature extractor with supervision, and then *re-trains the classifier with class-aware resampled loss*. Note that CRT is performing better than Supervised, indicating that the composition of the head and features learned from supervised learning is more sensitive to imbalanced dataset than the quality of feature extractor itself.

Even with a simple pre-training and fine-tuning pipeline, MoCo V2 representations can be comparable with much more complicated state-of-the-arts tailored to supervised imbalanced recognition, further corroborating the power of SSL under class imbalance. With rwSAM, we can further improve the result of MoCo V2.

Table 3: ImageNet-LT with Supervision.

Method	Backbone	Acc.
Supervised	ResNet-50	49.3
CRT [Kang et al., 2020]	ResNet-50	52.0
LADE [Hong et al., 2021]	ResNeXt-50	53.0
RIDE [Wang et al., 2021]	ResNet-50	54.9
RIDE [Wang et al., 2021]	ResNeXt-50	56.4
MoCo V2	ResNet-50	55.0
MoCo V2+rwSAM	ResNet-50	55.5

Table 4: Results of Pascal VOC Detection.

#Examples	116K	58K	14K
MoCo v2, balanced	78.3	76.5	74.3
MoCo v2, imbalanced	77.9	76.0	74.1
Supervised, balanced	74.8	71.4	61.0
Supervised, imbalanced	74.0	69.2	60.5

Algorithm 1 Reweighted Sharpness-Aware Minimization (rwSAM)

- 1: **Input:** the pre-training dataset $\widehat{\mathcal{D}}_s$.
- 2: **Output:** learned representations ϕ .
- 3: **Stage 1:** compute the weight w .
- 4: **for** $i = 0$ **to** **MaxIter** **do**
- 5: Randomly sample a batch of examples $\{x_i\}_{i=1}^b$ from $\widehat{\mathcal{D}}_s$.
- 6: Update the representations ϕ on $\{x_i\}_{i=1}^b$ to minimize the loss.

$$\phi \leftarrow \phi - \eta \nabla_{\phi} \widehat{L}(\phi).$$

- 7: **end for**
- 8: Generate the weight with kernel density estimation:

$$w_i = \left(\frac{1}{n} \sum_{j=1}^n K(f_{\phi}(x_i) - f_{\phi}(x_j), h) \right)^{-\alpha}.$$

- 9: **Stage 1:** reweighted SAM.
- 10: **for** $i = 0$ **to** **MaxIter** **do**
- 11: Randomly sample a batch of examples $\{x_i\}_{i=1}^b$ from $\widehat{\mathcal{D}}_s$.
- 12: Calculate $\epsilon(\phi)$ based on the reweighted loss $\widehat{L}_w(\phi)$.

$$\epsilon_{\phi} = \rho \operatorname{sgn}(\nabla_{\phi} \widehat{L}_w(\phi)) \left| \nabla_{\phi} \widehat{L}_w(\phi) \right|^{q-1} / \left(\|\nabla_{\phi} \widehat{L}_w(\phi)\|_q^q \right)^{1/p}$$

- 13: Update the representations ϕ on $\{x_i\}_{i=1}^b$ to minimize the loss and penalize the sharpness,

$$\phi \leftarrow \phi - \eta \nabla_{\phi} \widehat{L}(\phi + \epsilon(\phi)).$$

- 14: **end for**
-

We also test the performance of SSL with detection downstream tasks. We still consider MoCo v2 and ImageNet-LT following the setting of Section 2.2. During fine-tuning, we train the models on PascalVOC 07 and PascalVOC 12 training set and test on the PascalVOC 07 test set following the MoCo and SimCLR paper. As shown in Table 4, the gap between imbalance and balanced pertaining with MoCo is much smaller than the gap with supervised learning across all numbers of examples. SSL is still more robust to dataset class imbalance when the downstream task is detection.

D Proof of Theorem 3.1

We notate data from the first class as $x_i^{(1)} = e_1 - q_i^{(1)}\tau e_2 + \rho\xi_i^{(1)}$ where $i \in [n_1]$ and $q_i^{(1)} \in \{0, 1\}$. Similarly, we notate data from the second class as $x_i^{(2)} = -e_1 - q_i^{(2)}\tau e_2 + \rho\xi_i^{(2)}$ where $i \in [n_2]$ and $q_i^{(1)} \in \{0, 1\}$. We notate data from the third class as $x_i^{(3)} = e_2 + \rho\xi_i^{(3)}$ where $i \in [n_3]$. Notice that all $\xi_i^{(k)}$ are independently sampled from $\mathcal{N}(0, I)$.

We first introduce the following lemma, which gives some high probability properties of independent Gaussian random variables.

Lemma D.1. *Let $\xi_i \sim \mathcal{N}(0, I)$ for $i \in [n]$. Then, for any $n \leq \text{poly}(d)$, with probability at least $1 - e^{-d^{\frac{1}{10}}}$ and large enough d , we have:*

- $|\langle \xi_i, e_1 \rangle| \leq d^{\frac{1}{10}}$, $|\langle \xi_i, e_2 \rangle| \leq d^{\frac{1}{10}}$ and $|\|\xi_i\|_2^2 - d| \leq 4d^{\frac{3}{4}}$ for all $i \in [n]$.
- $|\langle \xi_i, \xi_j \rangle| \leq 3d^{\frac{3}{5}}$ for all $i \neq j$.

Proof of Lemma D.1. Let $\xi, \xi' \sim \mathcal{N}(0, I)$ be two independent random variables. By the tail bound of normal distribution, we have

$$\Pr\left(|\langle \xi, e_1 \rangle| \geq d^{\frac{1}{10}}\right) \leq d^{-\frac{1}{10}} \cdot e^{-\frac{d^{\frac{1}{5}}}{2}}. \quad (4)$$

By the tail bound of χ_d^2 distribution, we have

$$\Pr\left(|\|\xi\|_2^2 - d| \geq 4d^{\frac{3}{4}}\right) \leq 2e^{-\sqrt{d}}. \quad (5)$$

Since the directions of ξ and ξ' are independent, we can bound their correlation with the norm of ξ times the projection of ξ' onto ξ :

$$\Pr\left(|\langle \xi, \xi' \rangle| \geq 3d^{\frac{3}{5}}\right) \leq \Pr\left(\|\xi\|_2 \geq \sqrt{d} + 2d^{\frac{3}{5}}\right) + \Pr\left(|\langle \xi', \frac{\xi}{\|\xi\|} \rangle| \geq d^{\frac{1}{10}}\right) \leq \frac{e^{-\frac{d^{\frac{1}{5}}}{2}}}{d^{\frac{1}{10}}} + 2e^{-\sqrt{d}}. \quad (6)$$

Since every ξ_i and ξ_j are independent when $i \neq j$, by the union bound, we know that with probability at least $1 - (n^2 + 2n)\left(\frac{e^{-\frac{d^{\frac{1}{5}}}{2}}}{d^{\frac{1}{10}}} + 2e^{-\sqrt{d}}\right)$, we have $|\langle \xi_i, e_1 \rangle| \leq d^{\frac{1}{10}}$, $|\langle \xi_i, e_2 \rangle| \leq d^{\frac{1}{10}}$ and $|\|\xi_i\|_2^2 - d| \leq 4d^{\frac{3}{4}}$ for all $i \in [n]$, and also $|\langle \xi_i, \xi_j \rangle| \leq 3d^{\frac{3}{5}}$ for all $i \neq j$. Since the error probability is exponential in d , for large enough d , the error probability is smaller than $e^{-d^{\frac{1}{10}}}$, which finishes the proof. \square

Using the above lemma, we can prove the following lemma which constructs a linear classifier of the empirical dataset with relatively large margin and small norm.

Lemma D.2. *In the setting of Theorem 3.1, let $w_1^* = e_1$, $w_2^* = -e_1$, $w_3^* = \frac{1}{\rho d} \sum_{i=1}^{n_3} \xi_i^{(3)}$. Apply Lemma D.1 to the set of all $\xi_i^{(k)}$ where $k \in [3]$ and $i \in [n_k]$. When the high probability outcome of Lemma D.1 happens, the margin of classifier $\{w_1^*, w_2^*, w_3^*\}$ is at least $1 - O(d^{-\frac{1}{10}})$. Furthermore, we have $\|w_3^*\|_2^2 \leq O(d^{-\frac{1}{5}})$.*

Proof of Lemma D.2. When the high probability outcome of Lemma D.1 happens, we give a lower bound on the margin for all data in the dataset. For data $x = x_i^{(1)}$ in class 1, we have

$$w_1^{*\top} x = 1 + \langle \xi_i^{(1)}, e_1 \rangle \rho \geq 1 - \rho d^{\frac{1}{10}}, \quad (7)$$

$$w_2^{*\top} x = -1 + \langle \xi_i^{(1)}, e_1 \rangle \rho \leq -1 + \rho d^{\frac{1}{10}}, \quad (8)$$

$$w_3^{*\top} x = \frac{1}{\rho d} \left(e_1 - q_i^{(1)} \tau e_2 + \rho \xi_i^{(1)} \right)^\top \left(\sum_{j=1}^{n_3} \xi_j^{(3)} \right) \leq \frac{n_3(\tau+1)}{\rho d} d^{\frac{1}{10}} + \frac{3n_3}{d} d^{\frac{3}{5}}. \quad (9)$$

So the margin on data $(x_i^{(1)}, 1)$ is

$$w_1^{*\top} x - w_3^{*\top} x \geq 1 - \rho d^{\frac{1}{10}} - \frac{n_3(\tau+1)}{\rho d} d^{\frac{1}{10}} - \frac{3n_3}{d} d^{\frac{3}{5}} \geq 1 - O(d^{-\frac{1}{10}}). \quad (10)$$

Similarly, for data $x_i^{(2)}$ in class 2, the margin is at least $1 - O(d^{-\frac{1}{10}})$.

For data $x = x_i^{(3)}$ in class 3, we have

$$w_3^{*\top} x = \frac{1}{\rho d} \left(\sum_{j=1}^{n_3} \xi_j^{(3)} \right)^\top \left(e_2 + \rho \xi_i^{(3)} \right) \geq \frac{1}{d} \|\xi_i^{(3)}\|_2^2 - \frac{3n_3}{d} d^{\frac{3}{5}} - \frac{n_3 d^{\frac{1}{10}}}{\rho d} \geq 1 - O(d^{-\frac{1}{5}}). \quad (11)$$

On the other hand,

$$w_1^{*\top} x = \langle \rho \xi_i^{(3)}, e_1 \rangle \leq \rho d^{\frac{1}{10}}, \quad (12)$$

$$w_2^{*\top} x = \langle \rho \xi_i^{(3)}, -e_1 \rangle \leq \rho d^{\frac{1}{10}}. \quad (13)$$

So the margin is

$$w_3^{*\top} x - \max\{w_1^{*\top} x, w_2^{*\top} x\} \geq w_3^{*\top} x - \rho d^{\frac{1}{10}} \geq 1 - O(d^{-\frac{1}{10}}). \quad (14)$$

Finally, noticing that $\|w_3^*\|_2 \leq \frac{2n_3\sqrt{d}}{\rho d} \leq 2d^{-\frac{1}{10}}$ finishes the proof. \square

We also introduce the following helper lemma:

Lemma D.3. *Let $W \in \mathbb{R}^{3 \times d}$ be an arbitrary matrix, $m \geq 3$. Then, we have*

$$\|W\|_F^2 = \frac{1}{2} \min_{W_2 W_1 = W} (\|W_2^\top W_2\|_F^2 + \|W_1 W_1^\top\|_F^2), \quad (15)$$

where $W_1 \in \mathbb{R}^{m \times d}$ and $W_2 \in \mathbb{R}^{3 \times m}$. Furthermore, the minimum is achieved when $W_1 W_1^\top = W_2^\top W_2$.

Proof. On one hand, we have

$$\|W\|_F^2 = \text{Tr}(W W^\top) \quad (16)$$

$$= \min_{W_2 W_1 = W} \text{Tr}(W_2 W_1 W_1^\top W_2^\top) \quad (17)$$

$$= \min_{W_2 W_1 = W} \text{Tr}(W_1 W_1^\top W_2^\top W_2) \quad (18)$$

$$\leq \frac{1}{2} \min_{W_2 W_1 = W} (\|W_1 W_1^\top\|_F^2 + \|W_2^\top W_2\|_F^2), \quad (19)$$

where the inequality becomes equality if and only if $W_1 W_1^\top = W_2^\top W_2$.

On the other hand, let $W = U \Sigma V$ be the SVD decomposition of W , where $\Sigma \in \mathbb{R}^{3 \times d}$ is a diagonal matrix with $\sigma_1, \sigma_2, \sigma_3$ on its diagonal. For integers $p, q \geq 3$, we use $\Sigma_{p \times q}^{\frac{1}{2}}$ to denote the $p \times q$ matrix with $\sqrt{\sigma_1}, \sqrt{\sigma_2}, \sqrt{\sigma_3}$ at its first 3 diagonal positions and 0 otherwise. If we set $W_1 = \Sigma_{m \times d}^{\frac{1}{2}} V$ and $W_2 = U \Sigma_{3 \times m}^{\frac{1}{2}}$, then it can be verified that $W = W_2 W_1$ and $\|W\|_F^2 = \frac{1}{2} (\|W_1 W_1^\top\|_F^2 + \|W_2^\top W_2\|_F^2)$. Therefore, the equality holds in Equation 19, which finishes the proof. \square

Now we are ready to prove the supervised learning part of Theorem 3.1:

Proof of Theorem 3.1 (supervised learning part). Let $\{\hat{w}_1, \hat{w}_2, \hat{w}_3\}$ be three vectors in \mathbb{R}^d that minimize $\|w_1\|_2^2 + \|w_2\|_2^2 + \|w_3\|_2^2$ subject to the margin constraint $w_y^\top x \geq w_{y'}^\top x + 1$ for all empirical data (x, y) and $y' \neq y$. To prove the supervised learning part of Theorem 3.1, we will first prove that $\langle \hat{w}_1, e_1 \rangle^2 + \langle \hat{w}_2, e_1 \rangle^2 + \langle \hat{w}_3, e_1 \rangle^2 \leq O(d^{-\frac{1}{10}})$ with high probability, and then use this result to prove the correlation between e_2 and W_{SL} .

We first apply Lemma D.1 to the set of all $\xi_i^{(k)}$ where $k \in [3]$ and $i \in [n_k]$. We consider the situation when the high probability outcome of Lemma D.1 holds (which happens with probability at least $1 - e^{-d^{\frac{1}{10}}}$). By Lemma D.2, the constructed classifier $\{w_1^*, w_2^*, w_3^*\}$ has margin $\alpha \geq 1 - O(d^{-\frac{1}{10}})$ in this case. As a result, $\{\frac{1}{\alpha}w_1^*, \frac{1}{\alpha}w_2^*, \frac{1}{\alpha}w_3^*\}$ is a classifier with margin 1 and norm bounded by

$$\|\frac{1}{\alpha}w_1^*\|_2^2 + \|\frac{1}{\alpha}w_2^*\|_2^2 + \|\frac{1}{\alpha}w_3^*\|_2^2 = \frac{2 + \|w_3^*\|_2^2}{\alpha^2} \leq 2 + O(d^{-\frac{1}{10}}). \quad (20)$$

Let $\{\hat{w}_1, \hat{w}_2, \hat{w}_3\}$ be min-norm linear classifier of the empirical dataset. Since its norm cannot be larger than the constructed one, we have $\|\hat{w}_1\|_2^2 + \|\hat{w}_2\|_2^2 + \|\hat{w}_3\|_2^2 \leq 2 + O(d^{-\frac{1}{10}})$. By standard concentration inequality, when $n_1 \geq \text{poly}(d)$, with probability at least $1 - e^{-d^{\frac{1}{10}}}$, we have

$$\left| \mathbb{E}_{i \in [n_1], q_i^{(1)}=0} [x_i^{(1)}] - e_1 \right| \leq d^{-\frac{1}{10}}, \quad (21)$$

where the expectation is over all the data from class 1 that satisfies $q_i^{(1)} = 0$. By the definition of $\{\hat{w}_1, \hat{w}_2, \hat{w}_3\}$ we know $(\hat{w}_1 - \hat{w}_3)^\top x_i^{(1)} \geq 1$ for all $i \in [n_1]$, hence averaging over all the class 1 data with $q_i^{(1)} = 0$ and using the above inequality gives us

$$(\hat{w}_1 - \hat{w}_3)^\top e_1 \geq 1 - \|\hat{w}_1 - \hat{w}_3\|_2 \cdot d^{-\frac{1}{10}} \geq 1 - O(d^{-\frac{1}{10}}). \quad (22)$$

A similar analysis for class 2 data gives us

$$(\hat{w}_2 - \hat{w}_3)^\top (-e_1) \geq 1 - O(d^{-\frac{1}{10}}). \quad (23)$$

Now we prove that $\hat{w}_1, \hat{w}_2, \hat{w}_3$ all have small correlation with e_2 . Without loss of generality, we assume $\hat{w}_3^\top e_1 \triangleq t \geq 0$. If $t \geq \frac{1}{2}$, we have

$$\langle \hat{w}_1, e_1 \rangle^2 + \langle \hat{w}_2, e_1 \rangle^2 + \langle \hat{w}_3, e_1 \rangle^2 \geq \left(t + 1 - O(d^{-\frac{1}{10}}) \right)^2 > 2.25 - O(d^{-\frac{1}{10}}), \quad (24)$$

which contradicts with $\|\hat{w}_1\|_2^2 + \|\hat{w}_2\|_2^2 + \|\hat{w}_3\|_2^2 \leq 2 + O(d^{-\frac{1}{10}})$. Therefore, there must be $t \leq \frac{1}{2}$, hence

$$\langle \hat{w}_1, e_1 \rangle^2 + \langle \hat{w}_2, e_1 \rangle^2 + \langle \hat{w}_3, e_1 \rangle^2 \quad (25)$$

$$\geq \left(1 + t - O(d^{-\frac{1}{10}}) \right)^2 + \left(1 - t - O(d^{-\frac{1}{10}}) \right)^2 + t^2 \quad (26)$$

$$\geq 2 + 3t^2 - O(d^{-\frac{1}{10}}) \quad (27)$$

$$\geq 2 - O(d^{-\frac{1}{10}}). \quad (28)$$

As a result,

$$\langle \hat{w}_1, e_2 \rangle^2 + \langle \hat{w}_2, e_2 \rangle^2 + \langle \hat{w}_3, e_2 \rangle^2 \quad (29)$$

$$\leq \|\hat{w}_1\|_2^2 + \|\hat{w}_2\|_2^2 + \|\hat{w}_3\|_2^2 - \langle \hat{w}_1, e_1 \rangle^2 - \langle \hat{w}_2, e_1 \rangle^2 - \langle \hat{w}_3, e_1 \rangle^2 \quad (30)$$

$$\leq \left(2 + O(d^{-\frac{1}{10}}) \right) - \left(2 - O(d^{-\frac{1}{10}}) \right) \quad (31)$$

$$\leq O(d^{-\frac{1}{10}}). \quad (32)$$

Now we turn to the analysis of W_{SL} . Recall that we learn two matrices $W_1 \in \mathbb{R}^{m \times d}$ and $W_2 \in \mathbb{R}^{3 \times m}$ that minimize $\|W_1^\top W_1\|_F^2 + \|W_2^\top W_2\|_F^2$ subject to the margin constraint $(W_2 W_1 x)_y \geq (W_2 W_1 x)_{y'} + 1$, and the supervised representation is $W_{\text{SL}} = W_1$. According to Lemma D.3, we know that the solution W_1 and W_2 satisfy $W_2 W_1 = [\hat{w}_1, \hat{w}_2, \hat{w}_3]^\top$ and $W_2^\top W_2 = W_1 W_1^\top$. Let $W_2^\top W_2 = W_1 W_1^\top = U^\top \Sigma U$ be the SVD decomposition, where $\Sigma \in \mathbb{R}^{m \times m}$ is a non-negative diagonal matrix and U is a unitary matrix. Since W_2 has rank at most 3, there are at most 3 entries in Σ that are non-zero. Without loss of generality, we assume that all the non-zero entries of Σ are in the first 3 rows.

Let $\Sigma_{m \times d}$ and $\Sigma_{3 \times m}$ be the matrices by reshaping Σ (deleting or padding all-0 rows/columns) to the corresponding dimensions. We can write W_1 as $W_1 = U^\top \Sigma_{m \times d}^{\frac{1}{2}} V_1$ for some unitary matrix $V_1 \in \mathbb{R}^{d \times d}$, where $\Sigma_{m \times d}^{\frac{1}{2}}$ is the element-wise square root of $\Sigma_{m \times d}$. Similarly, $W_2 = V_2 \Sigma_{3 \times m}^{\frac{1}{2}} U$ for some unitary matrix $V_2 \in \mathbb{R}^{3 \times 3}$. Taking the product gives $W_2 W_1 = V_2 \Sigma_{3 \times d} V_1$.

Let $W_{\text{SL}} = W_1 = [w_1, w_2, \dots, w_m]^\top$. Now we finish the proof with

$$\sum_{i=1}^m \langle w_i, e_2 \rangle^2 = \|W_1 e_2\|_2^2 = \|U^\top \Sigma_{m \times d}^{\frac{1}{2}} V_1 e_2\|_2^2 \leq \|V_1 e_2\|_2^2 \cdot \|\Sigma_{d \times d} V_1 e_2\|_2^2 = \|V_2 \Sigma_{3 \times d} V_1 e_2\|_2^2 \quad (33)$$

$$= \|W_2 W_1 e_2\|_2^2 = \langle \hat{w}_1, e_2 \rangle^2 + \langle \hat{w}_2, e_2 \rangle^2 + \langle \hat{w}_3, e_2 \rangle^2 \leq O(d^{-\frac{1}{10}}). \quad (34)$$

□

To prove the self-supervised learning part of Theorem 3.1, we first introduce the following lemma which gives some helpful properties of the empirical data matrix.

Lemma D.4. *In the setting of Theorem 3.1, let $M \triangleq \mathbb{E}_x[xx^\top]$ where the expectation is over empirical data. Then, when $n_1, n_2 \geq \text{poly}(d)$, with probability at least $1 - e^{-d^{\frac{1}{10}}}$, we have: (1) $e_2^\top M e_2 \geq \Omega(d^{\frac{2}{5}})$, and (2) $u^\top M u \leq O(1)$ for all $u \in \mathbb{R}^d$ such that $u^\top e_2 = 0$ and $\|u\|_2 = 1$.*

Proof of Lemma D.4. Let $n = n_1 + n_2 + n_3$. We abuse notation and let ξ_i ($i \in [n]$) be the set of all $\xi_i^{(k)}$ that appears in the empirical data. Let matrix $M' = \frac{1}{n} \sum_{i=1}^n \xi_i \xi_i^\top$. By standard concentration inequalities and union bound, for $n \geq \text{poly}(d)$, with probability at least $1 - \frac{1}{2} e^{-d^{\frac{1}{10}}}$, we have that $|M'_{i,j}| \leq \frac{1}{d}$ for all $i \neq j$ and $|M'_{i,i} - 1| \leq \frac{1}{d}$ for all $i \in [d]$. In this case, for any vector $u \in \mathbb{R}^d$ such that $\|u\|_2 = 1$ and $u^\top e_2 = 0$, we have

$$u^\top M u \leq 2\|u\|_2^2 + 2u^\top (\rho^2 M') u \leq 2 + 2\rho^2 + 2\rho^2 \|M' - I\|_F \leq O(1). \quad (35)$$

On the other hand, by the definition of data distribution and standard concentration inequalities, for $n \geq \text{poly}(d)$, with probability at least $1 - \frac{1}{2} e^{-d^{\frac{1}{10}}}$ we have that: at least $\frac{1}{3}$ of all data either is class 1 with $q_i^{(1)} = 1$ or class 2 with $q_i^{(2)} = 1$, and $\|\frac{1}{n} \sum_{i=1}^n \xi_i\|_2 \leq O(\frac{1}{d})$. In this case,

$$e_2^\top M e_2 = \mathbb{E}_x[(e_2^\top x)^2] \geq (\mathbb{E}_x[e_2^\top x])^2 \geq \left(\frac{1}{3} \tau - e_2^\top \left(\frac{1}{n} \sum_{i=1}^n \xi_i \right) \right)^2 \geq \Omega(\tau^2) = \Omega(d^{\frac{2}{5}}). \quad (36)$$

□

Using the above lemma, we can prove the self-supervised learning part of Theorem 3.1.

Proof of Theorem 3.1 (self-supervised learning part). Let $M = \mathbb{E}_x[xx^\top]$ be the empirical data matrix, where the expectation is over the dataset. Notice that self-supervised learning objective has the same minimizer as the matrix factorization objective $\|M - W^\top W\|_F^2$, by Eckart–Young–Mirsky theorem we know that the span of $\tilde{w}_1, \tilde{w}_2, \dots, \tilde{w}_m$ is exactly the span of the top m eigenvectors of matrix M . Let $M = \sum_{i=1}^d \lambda_i v_i v_i^\top$ where λ_i is the i -th largest eigenvalue of M with the corresponding eigenvector v_i . We decompose e_2 in the eigenvector basis as $e_2 = \sum_{i=1}^d \zeta_i v_i$.

We first note that $\lambda_1 \geq \Omega(d^{\frac{2}{5}})$ and $\max_{i \neq 1} \lambda_i \leq O(1)$. Indeed, we know that $\mathbb{E}[M] = \text{diag}(1 + d^{-\frac{2}{5}}, d^{\frac{2}{5}} + d^{-\frac{2}{5}}, d^{-\frac{2}{5}}, \dots, d^{-\frac{2}{5}})$. By standard matrix concentration bounds (e.g. Theorem 4.6.1 of Vershynin [2018]), we know that with probability at least $1 - e^{-d^{\frac{1}{10}}}$, $\|M - \mathbb{E}[M]\| \leq O(d^{-\frac{2}{5}})$. By Weyl's inequality we know that $\max_i |\lambda_i(T) - \lambda_i(S)| \leq \|S - T\|$, so $\lambda_1 \geq \Omega(d^{\frac{2}{5}})$ and $\max_{i \neq 1} \lambda_i \leq O(1)$.

By Lemma D.4, we know that with probability at least $1 - e^{-d^{\frac{1}{10}}}$, we have $e_2^\top M e_2 \geq \Omega(d^{\frac{2}{5}})$ and $\frac{u^\top M u}{\|u\|_2^2} \leq O(1)$ for all u orthogonal to e_2 . To prove the result regarding self-supervised learning, we only need to prove that $\zeta_1^2 \geq 1 - O(d^{-\frac{1}{5}})$ in this case.

We first show that $\zeta_1^2 \geq \frac{1}{2}$. For contradiction, first assume $\zeta_1^2 \leq \frac{1}{2}$. Define vector

$$u = \sqrt{1 - \zeta_1^2} v_1 - \frac{\zeta_1 \sum_{i=2}^d \zeta_i v_i}{\sqrt{1 - \zeta_1^2}}. \quad (37)$$

which satisfies $u^\top e_2 = 0$ and $\|u\|_2^2 = 1$. Notice that

$$\frac{u^\top M u}{\|u\|_2^2} = (1 - \zeta_1^2) \lambda_1 - \frac{\zeta_1^2 \sum_{i=2}^d \zeta_i^2 \lambda_i}{1 - \zeta_1^2} \quad (38)$$

$$\geq \frac{\lambda_1}{2} - \max_{i \neq 1} \lambda_i \quad (39)$$

$$\geq \Omega(d^{\frac{2}{5}}), \quad (40)$$

which contradicts to $\frac{u^\top M u}{\|u\|_2^2} \leq O(1)$. Therefore, we have $\zeta_1^2 \geq \frac{1}{2}$.

To prove that ζ_1^2 is close to 1, we let scalar $t = \frac{1}{\zeta_1^2} - 1$ and define vector

$$u = -t \zeta_1 v_1 + \sum_{i=2}^d \zeta_i v_i, \quad (41)$$

which satisfies $u^\top e_2 = 0$. Since $\zeta_1^2 \geq \frac{1}{2}$, we have $t \leq 1$ and $\|u\|_2^2 \leq 1$. As a result, we have

$$\frac{u^\top M u}{\|u\|_2^2} \geq t^2 \lambda_1 \zeta_1^2 + \sum_{i=2}^d \lambda_i \zeta_i^2 \geq t^2 e_2^\top M e_2 \geq \Omega(t^2 d^{\frac{2}{5}}). \quad (42)$$

On the other hand, we know that $\frac{u^\top M u}{\|u\|_2^2} \leq O(1)$. Comparing these two bounds gives us $t^2 \leq O(d^{-\frac{1}{5}})$, which means $\zeta_1^2 \geq 1 - O(d^{-\frac{1}{5}})$. \square